Ferroelectricity emerging in strained (111)-textured ZrO2 thin films

Zhen Fan, Jinyu Deng, Jingxian Wang, Ziyan Liu, Ping Yang, Juanxiu Xiao, Xiaobing Yan, Zhili Dong, John Wang, and Jingsheng Chen

Citation: Applied Physics Letters **108**, 012906 (2016); doi: 10.1063/1.4939660
View online: http://dx.doi.org/10.1063/1.4939660
View Table of Contents: http://scitation.aip.org/content/aip/journal/apl/108/1?ver=pdfcov
Published by the AIP Publishing

Ferroelectricity emerging in strained (111)-textured ZrO_2 thin films

Zhen Fan,[1,a)] Jinyu Deng,[1] Jingxian Wang,[2] Ziyan Liu,[1] Ping Yang,[3] Juanxiu Xiao,[1] Xiaobing Yan,[1] Zhili Dong,[2] John Wang,[1] and Jingsheng Chen[1,a)]
[1]*Department of Materials Science and Engineering, National University of Singapore, 9 Engineering Drive 1, Singapore 117575, Singapore*
[2]*School of Materials Science and Engineering, Nanyang Technological University, Nanyang Avenue, Singapore 639798, Singapore*
[3]*Singapore Synchrotron Light Source, National University of Singapore, 5 Research Link, Singapore 117603, Singapore*

(Received 22 October 2015; accepted 26 December 2015; published online 7 January 2016)

(Anti-)ferroelectricity in complementary metal-oxide-semiconductor (CMOS)-compatible binary oxides have attracted considerable research interest recently. Here, we show that by using substrate-induced strain, the orthorhombic phase and the desired ferroelectricity could be achieved in ZrO_2 thin films. Our theoretical analyses suggest that the strain imposed on the ZrO_2 (111) film by the TiN/MgO (001) substrate would energetically favor the tetragonal (t) and orthorhombic (o) phases over the monoclinic (m) phase of ZrO_2, and the compressive strain along certain ⟨11-2⟩ directions may further stabilize the o-phase. Experimentally ZrO_2 thin films are sputtered onto the MgO (001) substrates buffered by epitaxial TiN layers. ZrO_2 thin films exhibit t- and o-phases, which are highly (111)-textured and strained, as evidenced by X-ray diffraction and transmission electron microscopy. Both polarization-electric field (*P-E*) loops and corresponding current responses to voltage stimulations measured with appropriate applied fields reveal the ferroelectric sub-loop behavior of the ZrO_2 films at certain thicknesses, confirming that the ferroelectric o-phase has been developed in the strained (111)-textured ZrO_2 films. However, further increasing the applied field leads to the disappearance of ferroelectric hysteresis, the possible reasons of which are discussed. © *2016 AIP Publishing LLC*. [http://dx.doi.org/10.1063/1.4939660]

Since the first demonstration of ferroelectricity in a 10-nm-thick Si-doped HfO_2 thin film in the year of 2011,[1] there has been a flurry of interests from the ferroelectric community in studying HfO_2 and its analogue, ZrO_2. These simple binary oxides are highly expected to overcome the complementary metal-oxide-semiconductor (CMOS)-integration and scaling issues suffered by conventional perovskite ferroelectrics for the applications of ferroelectric random access memory (FeRAM).[2,3] It has been reported that ferroelectricity or antiferroelectricity can exist in a wide spectrum of HfO_2-based thin films, either undoped[4] or with various dopants, such as Si,[1,5–7] Zr,[8–13] Y,[14–17] Al,[18] Gd,[19] and Sr.[20] The origin of (anti-)ferroelectricity in HfO_2-based thin films has been further revealed to be due to the formation of a polar, orthorhombic $Pca2_1$ phase (o-phase). However, compared to HfO_2, ZrO_2 has received much less research attention in terms of (anti-)ferroelectricity. Indeed, it was just in Mg-doped ZrO_2 where the o-phase was first discovered, although its ferroelectric-related properties were not studied in that early work.[21] It was only recently that antiferroelectric double-hysteresis loops were observed in pure ZrO_2 thin films, indicating that ZrO_2 underwent an electric field-driven phase transition from tetragonal ($P4_2/nmc$; nonpolar) to orthorhombic.[8] A later theoretical work demonstrated that a small energy difference of 1 meV/f.u. between the tetragonal (t-) and o-structures was the key underlying the observed antiferroelectricity.[22] While the appearance of t → o phase transition under electric field (i.e., antiferroelectricity) in ZrO_2 thin films seems to be interesting, the stabilization of the o-phase during film growth remains difficult and there has been no direct evidence of ferroelectricity associated with the o-ZrO_2 reported so far. Therefore, in this work, we aim to explore a way to stabilize the o-phase in ZrO_2 thin films and further demonstrate the ferroelectric behavior of this polar phase.

ZrO_2 has four major polymorphs: cubic ($Fm\text{-}3m$), monoclinic ($P2_1/c$), and aforementioned tetragonal and orthorhombic. In the ZrO_2 bulk, the monoclinic (m-) phase, which is the most stable phase at room temperature, transforms to t- and further to cubic (c-) phases, at about 1200 K and 2400 K, respectively.[23] In ZrO_2 polycrystalline thin films, on the other hand, the t-phase is more energetically stable than the m-phase due to the well-known surface energy effect,[24] which is strongly dependent on the crystal size and film thickness. The mechanisms of forming the o-phase, however, have not been completely understood. From the crystallographic viewpoint, the o-structure can be transformed from the t-structure by elongating the *c*-axis while shortening and differing the *a*- and *b*-axes of the t-structure. (tetragonal: $a = b = 5.09$ Å, $c = 5.18$ Å;[25] orthorhombic: $a = 5.26$ Å, $b = 5.07$ Å, and $c = 5.08$ Å.[21] By transformation, the *c*-axis of the t-structure becomes the *a*-axis of the o-structure, while the longer axis between *a*- and *b*-axes of the t-structure becomes the *c*-axis of the o-structure. The direction of *P*r of the o-phase is along its *c*-axis.) This phase transition requires asymmetric strain exerted on the t-structure, i.e., compressive strain within its *aob* plane and tensile strain along its

[a)]Authors to whom correspondence should be addressed. Electronic addresses: a0082709@u.nus.edu and msecj@nus.edu.sg.

c-axis. According to previous studies, the asymmetric strain in polycrystalline thin films can be caused by many factors, including thermal expansion mismatch,[21] doping,[18] surface energy effect,[24] island coalescence,[11] mechanical confinement from the capping layer,[1] and applying electric field.[8] Although all these factors are expected to induce the formation of the o-phase in ZrO_2 thin films, so far only the last factor has successfully led to the measurable ferroelectric-related properties, albeit antiferroelectricity. This fact indicates that the o-phase of ZrO_2 is rather difficult to be stabilized during film growth, and the ferroelectricity of this metastable phase needs to be proved more directly. Additional factors which can stabilize the o-ZrO_2 are therefore of great importance. Because previous studies were mainly focused on ZrO_2 polycrystalline thin films, there has been little chance for the substrate-induced strain to play a role in stabilizing the o-phase. The substrate-induced strain has been often employed in epitaxial and textured thin films to achieve the desired phases and corresponding properties. For example, ferroelectricity can be induced in $SrTiO_3$ (001) epitaxial thin films under biaxial tensile strain.[26] We therefore use the substrate-induced strain to stabilize the o-phase of ZrO_2 in this study.

The MgO (001) substrate and an epitaxially grown TiN electrode layer are selected for the growth of strained ZrO_2 films. A strain analysis was conducted for the ZrO_2 film grown on the TiN/MgO (001) substrate. For simplicity, all the ZrO_2 films with different phases are assumed to have the same (111)-orientation (Figure 1(a)), because (111) planes are the most energetically preferred planes for the growth of ZrO_2.[27] (The most preferable plane of m-ZrO_2 is (-111) if β is an obtuse angle, or (111) equivalently if β is an acute angle.) In fact, this assumption agrees well with our experimental results, which will be presented later. The most likely orientation relationship between of ZrO_2 (111) and TiN (001) planes is $ZrO_2\langle 1\text{-}10\rangle$//$TiN\langle 110\rangle$ (Figure 1(b)). Consequently, $ZrO_2\langle 11\text{-}2\rangle$//$TiN\langle 110\rangle$ is also established. This orientation relationship is deducible from the lattice matching and has been reported previously.[28] For example, $a_{\langle 1\text{-}10\rangle}$ and $a_{\langle 11\text{-}0\rangle}$ of c-ZrO_2 are 7.241 and 6.271 Å, respectively, which best matches two times of the lattice dimension along the $\langle 110\rangle$ direction of TiN ($2 \times 4.24/\sqrt{2} = 5.996$ Å). (Note that the structural parameters of c-, t-, m-, and o-phases for the strain analysis are collected from Refs. 29, 25, 30 and 21, respectively.) Then, the ZrO_2 (111) planes are further analyzed at the atomic level and only Zr atoms are used for analysis because they are heavy atoms compared with O. The (111) plane is constructed by two unit triangles with different orientations, i.e., upward and downward. For c- and t-structures, the dimension and the atomic configuration of upward and downward triangles are identical (Figures 1(c) and 1(d)). However, the situation is not the same in m- and o-structures (Figures 1(e) and 1(f)). One can see the motions of Zr atoms away from the centers of the triangle edges, and the motions are different in upward and downward triangles. These motions of Zr atoms may be favored or disfavored under the strain provided by the TiN underlayer. The strain state is evaluated by considering both the tensile/compressive and the shear deformations of the (111) triangles. More specifically, two parameters are defined: $\Delta a = |a_{\langle 1\text{-}10\rangle} - 5.996\,\text{Å}| + |a_{\langle 11\text{-}2\rangle} - 5.996\,\text{Å}|$ and $\Delta\alpha = |\alpha - 90^\circ|$, to estimate the levels of tensile/compressive and shear deformations, respectively. Here, if the Zr atoms along one triangle edge are not collinear, $a_{\langle 1\text{-}10\rangle}$ will be treated as the sum of the distances between two nearest neighboring Zr atoms (Figure 1(e)). As can be seen from Table S1,[31] the c- and t-structures have the smallest Δa_{avg} and $\Delta\alpha_{avg}$, indicating that they can best accommodate the strain. However, because the c-phase in pure ZrO_2 can exist only at high temperature, it will not be brought into further discussions regarding the film growth. Table S1 also shows that the o-structure has smaller Δa_{avg} and $\Delta\alpha_{avg}$ than the monoclinic counterpart,[31] suggesting that the o-structure is more favorable to accommodate the strain. From these results, one can further infer that during the growth of ZrO_2 thin films on TiN/MgO (001) substrates, the t-phase will dominate when the strain is considered. Also due to strain, the o-phase has priority over the m-phase to be formed. The suppression of the m-phase is one of the prerequisites of forming the o-phase. In addition, the o-structure has certain atomic distances which are quite close to 5.996 Å, such as $a_{[\text{-}211]}$ (6.019 Å) in the downward triangle and $a_{[1\text{-}21]}$ (6.117 Å) in the upward triangle.[31] This closeness found in the o-structure is even greater than that found in the t-structure, indicating that the o-phase is more favorable than the t-phase to accommodate the compressive strain along certain $\langle 11\text{-}2\rangle$ directions. This provides a driving force for the t → o phase transition and the stabilization of the o-phase. We speculate that the o-phase might be formed in some local regions, where the compressive strain along certain $\langle 11\text{-}2\rangle$ directions plays the dominate role while the strain along other directions has less effect due to strain relaxation along those directions. It should be emphasized that just because of the compressive strain along those $\langle 11\text{-}2\rangle$ directions, two Zr atoms in the downward and upward triangles (as marked in Figure 1(f)) undergo significant displacements along the *b* axis with however different signs (Figure

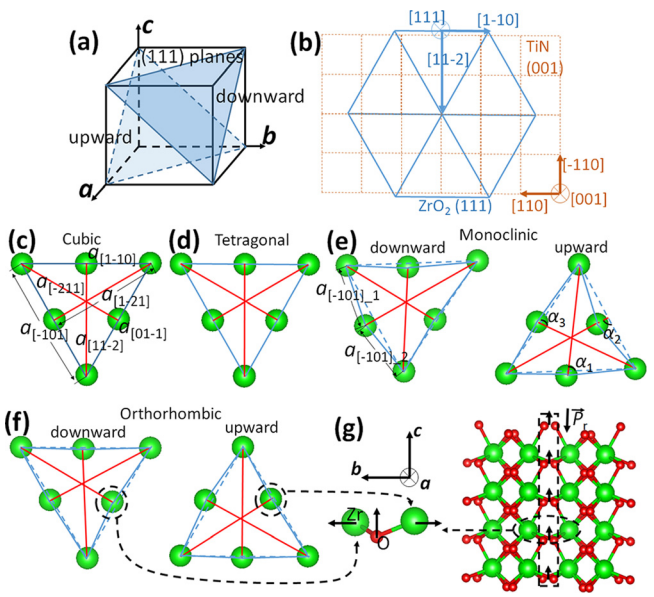

FIG. 1. Schematics showing: (a) (111) planes of ZrO_2 pseudo-cubic structure; (b) the theoretical orientation of the ZrO_2 (111) planes relative to the TiN (001) planes; unit triangles of (111) planes of (c) cubic, (d) tetragonal, (e) monoclinic and (f) orthorhombic phases; and (g) the atomic displacements of Zr and O in the o-phase.

1(g)). This *b*-axis motion of Zr atoms strongly pulls the O atoms up along the *c*-axis (Figure 1(g)), which is the origin of ferroelectric polarization. Up to this point, we have established the mechanism of how the strain stabilizes the o-phase and induces the ferroelectricity in ZrO_2 (111) thin films grown on TiN/MgO (001) substrates. We note that in the real films, there may not be a simple epitaxial relationship between (111)-ZrO_2 and (001)-TiN existing macroscopically, because to help release the strain, multiple phases can coexist and the lattice disorientations within the ZrO_2 (111) planes may occur. However, our theoretical model still applies in explaining how the strain stabilizes the o-phase of ZrO_2, provided that in certain local regions, the growth of ZrO_2 follows the orientation relationship of $ZrO_2\langle 1\text{-}10\rangle$//TiN$\langle 110\rangle$ and $ZrO_2\langle 11\text{-}2\rangle$// TiN$\langle 110\rangle$. We also note that in the modelling of the (111)-ZrO_2/(001)-TiN interface, anions and their bonding with cations at the interface and the partial oxidation of TiN[7,32] are neglected and the reasonability of these approximations is explained in the supplementary material.[31] Finally, the strain may not be the only factor of determining the formation of the o-ZrO_2, and other aforementioned factors may still work.

ZrO_2 thin films with different thicknesses of 8, 12, 18, and 24 nm were deposited on TiN-buffered MgO (001) substrates by rf-magnetron sputtering (AJA Orion 8). During the growth of both TiN and ZrO_2, the sputtering power, temperature, and argon gas pressure were kept at 200 W, 700 °C, and 10 mTorr, respectively. No postannealing treatment was adopted. The crystal structures of ZrO_2 thin films were studied using high-resolution X-ray diffraction (HRXRD; Huber four circle diffractometer system 90000-0216/0) with an X-ray wavelength of 1.4922 Å. Their microstructures were further examined by cross-sectional high-resolution transmission electron microscopy (HRTEM; JEOL JEM-2100F). Dielectric spectroscopy was performed using an impedance analyzer (Solartron 1260). DC leakage current was investigated using an electrometer (Keithley 6430). Polarization-electric field (*P*-*E*) hysteresis loops were measured with a ferroelectric test station (Radiant Precision Workstation). Au dots with diameters of 200 μm were sputtered onto the samples to function as top electrodes. The bias was applied to the top electrode.

Figure 2(a) shows the high-resolution θ-2θ scans of ZrO_2/TiN/MgO heterostructures with different layer thicknesses of ZrO_2. Strong TiN (002) peaks together with thickness fringes demonstrate the high-quality epitaxy of TiN grown on the MgO (001) substrate. The epitaxial relationship between TiN and MgO is further proved by the HRTEM image (Figure S1[31]). In 8- and 12-nm-thick ZrO_2 films, the major peak of ZrO_2 is identified as the t-/o-phase (111) peak (the $d_{(111)}$ values of t- and o-phases are extremely similar and thus their (111) peaks cannot be distinguished). In 18- and 24-nm-thick ZrO_2 films, however, the m-phase (-111) (or (111) equivalently if β is an acute angle) peak emerges and the peak intensity becomes higher when the film is thicker. It is also observed that the t-/o-phase (111) peak shifts from 28.50° to 28.60°, 28.70°, and 28.74° as the film thickness increases, corresponding to a shrinkage of the out-of-plane lattice spacing $d_{(111)}$ from 3.031 to 3.021, 3.011, and 3.006 Å. Considering that the conventional $d_{(111)}$ value of the t-/o-phase in polycrystalline ZrO_2 thin films is 2.96 Å,[10] it can be concluded that the (111)-textured ZrO_2 films are highly strained and the strain relaxes with the film thickness. Our X-ray diffraction (XRD) results therefore confirm our previous theoretical analyses, i.e., the substrate-induced strain will take effect in ZrO_2 thin films by promoting the stabilization of t- and o-phases while its relaxation leads to the emergence of the m-phase. Note again that other factors, such as the surface energy effect,[24] may also play a role in the stabilization of t- and o-phases.

To further investigate the film microstructure, cross-sectional HRTEM was conducted for a 12-nm-thick ZrO_2 film. The HRTEM image (Figure 2(b)) was taken when the incident beam was slightly tilted from the [110] zone axis of MgO, in order to make the incident beam coincide with the possible in-plane lattice vectors of ZrO_2. Due to the tilting and thickness issue, the very clear and ordered lattice fringes of MgO and TiN could hardly be observed, although the FFT patterns (Figure 2(b)) of the MgO/TiN interface (Zone 1) and the TiN film (Zone 2) already show the epitaxial growth of TiN on top of MgO. The cubic-on-cubic epitaxial relationship between TiN and MgO can be more apparently revealed by the HRTEM image taken in another thin region after properly aligning the sample (Figure S1[31]). Turning to the ZrO_2 layer, distinct lattice fringes perpendicular to the out-of-plane direction are clearly seen throughout the whole ZrO_2 film, indicating that the ZrO_2 film is highly textured. According to the FFT pattern (Figure 2(b)), the out-of-plane lattice spacing is calculated as 3.02 Å, which is consistent with the $d_{(111)}$ value of the t-/o-phase obtained from XRD. In certain local regions, e.g., Zone 3 in Figure 2(b), some weak lattice fringes perpendicular to the in-plane direction are observed. Based on the in-plane FFT spot (Figure 2(b)), the in-plane lattice spacing is calculated as ~1.78 Å, which corresponds to the spacing of (2-20) planes. The zone axis is therefore identified to be [11-2]. In addition to this set of lattice, another set of lattice with the [1-10] zone axis is also observed (see the FFT pattern of Zone 3 in Figure 2(b)). It is difficult to further identify which phase these two sets of lattices exactly belong to, because of the lack of complete

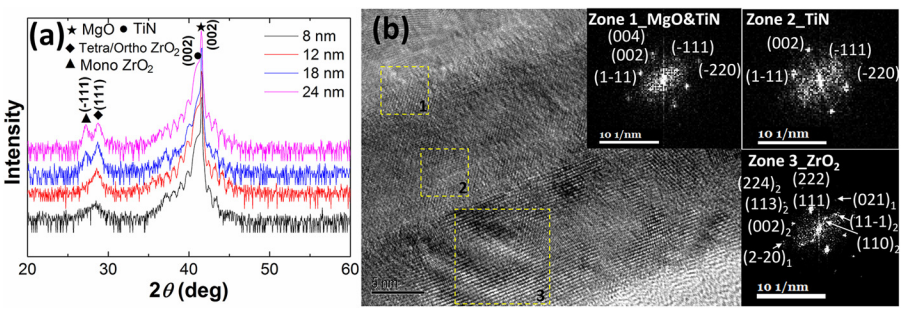

FIG. 2. (a) High-resolution θ-2θ scans of ZrO_2/TiN/MgO heterostructures with ZrO_2 thicknesses of 8, 12, 18, and 24 nm, respectively. (b) HRTEM image and corresponding FFT patterns of the ZrO_2/TiN/MgO heterostructure. The subscripts "1" and "2" in the FFT pattern of Zone 3 indicate two different sets of lattices with zone axes of [11-2] and [1-10], respectively.

lattice information. Nevertheless, these results demonstrate that in the local region, the in-plane orientation relationship of $ZrO_2\langle 1\text{-}10\rangle//TiN\langle 110\rangle$ and $ZrO_2\langle 11\text{-}2\rangle//TiN\langle 110\rangle$ is established. In addition, the slight tiling which allows the appearance of the in-plane lattice fringes of ZrO_2 indicates that $ZrO_2\langle 1\text{-}10\rangle$ (or $\langle 11\text{-}2\rangle$) is not rigorously parallel to $TiN\langle 110\rangle$. It should also be noted that the whole ZrO_2 film does not show in-plane lattice fringes similar to those in Zone 3 macroscopically, due to the coexist of multiple phases and the lattice disorientations within the ZrO_2 (111) planes. Our transmission electron microscopy (TEM) studies therefore reveal that the 12-nm-thick ZrO_2 film exhibits highly (111)-textured t-/o-phase, and that in certain local regions, the growth of ZrO_2 follows the orientation relationship of $ZrO_2\langle 1\text{-}10\rangle//TiN\langle 110\rangle$ and $ZrO_2\langle 11\text{-}2\rangle//TiN\langle 110\rangle$.

Now let us focus on the most concerned results of *P-E* hysteresis loops. Here, only the results of the 12-nm-thick film are presented (Figure 3) and those of other films can be found in the supplementary material.[31] The *P-E* loops exhibit the ferroelectric-like but leaky behavior when the applied field is below 2.08 MV/cm (Figure 3(a)). Further increasing the applied field to above 2.5 MV/cm, which is intended to saturate the loops, however, results in a vanishing of hysteresis (the reason will be discussed later). To evaluate the leakage contribution to the ferroelectric-like hysteresis, frequency dependent *P-E* loops are investigated (Figure 3(b)). The loops are not inflated significantly with decreasing the frequency, indicating that the leakage contribution is not large and the polarization after leakage compensation[33] will not be dramatically reduced. To gain more reliable evidence, current response to a voltage stimulation[34] is recorded and presented in Figure 3(c). It is observed that weak current peaks are located at the fields of 1.5–2.0 MV, indicating the occurrence of polarization switching. The tilting of current curves in the time regions of 0–0.025, 0.075–0.15, and 0.225–0.30 ms may well be caused by two factors: (1) leakage current; and (2) current due to the polarization switching and back-switching (the polarization back-switching is resulted from the polarization relaxation, and it is often seen in relaxor ferroelectrics[35,36]). If the leakage current in the *P-E* measurement is close to that measured with the DC method, its magnitude may thus be smaller than 10 μA at 2 MV/cm (Figure 3(d)). Therefore, the polarization switching and back-switching current can become the major contributor to the total current. The unsaturated polarization switching and subsequent back-switching will result in sub-loops, which may make the hysteresis loops look leaky.[37] On the basis of the above results, the ferroelectricity, albeit weak, has been confirmed in the 12-nm-thick ZrO_2 film (may also in the 18-nm-thick film[31]). Note that previous (111)-textured $Hf_{0.5}Zr_{0.5}O_2$ films grown on (111)-textured Pt substrates did not show any ferroelectricity,[11] which seems to be inconsistent with our results. The reason is that the strain in their films is isotropic, and thus, there is no driving force for the stabilization of the o-phase. In our (111)-textured ZrO_2 films grown on TiN/MgO (001) substrates, however, the strain is anisotropic and the compressive strain along certain $\langle 11\text{-}2\rangle$ directions can favor the formation of the o-phase, as discussed above. Next, we discuss the possible reasons of the disappearance of the ferroelectric hysteresis with the increasing applied field. The first possible reason is the phase transition from orthorhombic to tetragonal (and also to monoclinic) under large electric field. When large AC fields are applied along the [111] direction (i.e., the out-of-plane direction) of the ZrO_2 structure, the *a*, *b*, and *c* axes will deform simultaneously, including both tensile/compressive and shear deformations. Given the original ZrO_2 structure is orthorhombic, the simultaneous deformation of *a*, *b*, and *c* axes can eventually lead to the structural transformation from ferroelectric orthorhombic to paraelectric tetragonal (and also monoclinic), because the latter two are more energetically favorable. These paraelectric phases are considerably stable and they could not be transformed back to the ferroelectric phase even under the maximum allowed field (in our experiments, the (anti-)ferroelectric-like hysteresis could not revive even when the field is increased to the breakdown field). Another possible cause is the increased homogeneous space charge density under high electric field, which makes the hysteresis loop constricted or almost disappeared when the space charge density is large enough.[38] This is because the electric field formed by the space charge weakens the total electric field and thus it is not sufficient to saturate the polarization. Other factors which can hinder the motion of domains, such as microstructural evolution and redistribution of oxygen vacancies, may also be able to cause the disappearance of hysteresis under high electric field. The exact reason for the hysteresis disappearance deserves further investigation for confirmation (see more discussion in the supplementary material[31]). Nevertheless, the *P-E* hysteresis loops together with the current responses to voltage stimulations have already demonstrated the ferroelectricity in the strained (111)-textured ZrO_2 thin films.

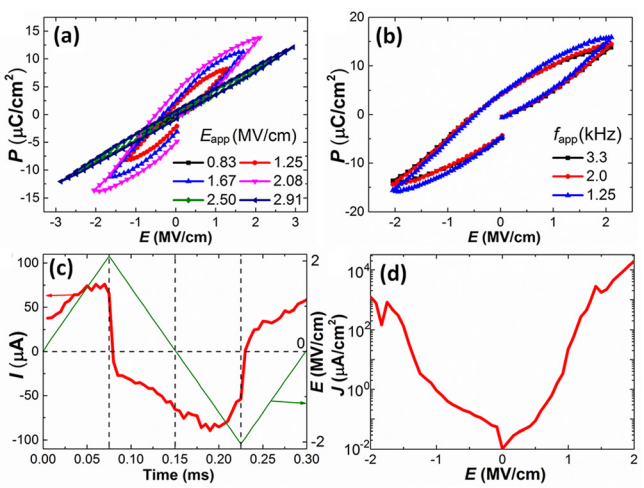

FIG. 3. (a) Electric field dependent ($f_{app} = 3.3$ kHz) and (b) frequency dependent ($E_{app} = 2.08$ MV/cm) *P-E* hysteresis loops, (c) current response to a voltage stimulation ($f_{app} = 3.3$ kHz, $E_{app} = 2.08$ MV/cm), and (d) DC leakage current of the 12-nm-thick ZrO_2 film.

In summary, we have demonstrated a way of using substrate-induced strain to stabilize the ferroelectric o-phase in ZrO_2 thin films. First, our theoretical analyses show that in ZrO_2 (111) films grown on TiN/MgO (001) substrates, the m-phase is energetically disfavored, and there is a tendency of structural transformation from tetragonal to orthorhombic due to the compressive strain imposed on certain $\langle 11\text{-}2\rangle$ directions in ZrO_2 (111) planes. Then, experimentally, ZrO_2

films are deposited on TiN-buffered MgO (001) substrates by sputtering. XRD and TEM results reveal the epitaxial nature of the TiN layer, and the strained t- and o-phases with the strong (111)-texture in ZrO_2 films. Both *P-E* hysteresis loops and current responses to voltage stimulations confirm the ferroelectricity in ZrO_2 films with certain thicknesses, evidencing that the ferroelectric o-phase has been achieved in the strained (111)-textured ZrO_2 films. The disappearance of ferroelectric hysteresis under high fields is observed and several plausible reasons are discussed. This study contributes an effective approach to stabilize the o-phase and achieve the ferroelectricity in ZrO_2 thin films, which may facilitate the development of new ferroelectric binary oxides for thin-film memories.

The research was supported by the Singapore National Research Foundation under CRP Award No. NRF-CRP10-2012-02. Z.F. thanks Dr. C. Tang for valuable discussions on TEM results.

[1]T. S. Böscke, J. Müller, D. Bräuhaus, U. Schröder, and U. Böttger, Appl. Phys. Lett. **99**, 102903 (2011).
[2]J. Müller, P. Polakowski, S. Mueller, and T. Mikolajick, ECS J. Solid State Sci. Technol. **4**, N30 (2015).
[3]M. H. Park, Y. H. Lee, H. J. Kim, Y. J. Kim, T. Moon, K. D. Kim, J. Müller, A. Kersch, U. Schröder, T. Mikolajick, and C. S. Hwang, Adv. Mater. **27**, 1811 (2015).
[4]P. Polakowski and J. Müller, Appl. Phys. Lett. **106**, 232905 (2015).
[5]T. S. Böscke, St. Teichert, D. Bräuhaus, J. Müller, U. Schröder, U. Böttger, and T. Mikolajick, Appl. Phys. Lett. **99**, 112904 (2011).
[6]D. Zhou, J. Müller, J. Xu, S. Knebel, D. Bräuhaus, and U. Schröder, Appl. Phys. Lett. **100**, 082905 (2012).
[7]D. Zhou, J. Xu, Q. Lu, Y. Guan, F. Cao, X. Dong, J. Müller, T. Schenk, and U. Schröder, Appl. Phys. Lett. **103**, 192904 (2013).
[8]J. Müller, T. S. Böscke, U. Schröder, S. Mueller, D. Bräuhaus, U. Böttger, L. Frey, and T. Mikolajick, Nano Lett. **12**, 4318 (2012).
[9]J. Müller, T. S. Böescke, D. Bräuhaus, U. Schröeder, U. Böttger, J. Sundqvist, P. Kücher, T. Mikolajick, and L. Frey, Appl. Phys. Lett. **99**, 112901 (2011).
[10]M. H. Park, H. J. Kim, Y. J. Kim, W. Lee, T. Moon, and C. S. Hwang, Appl. Phys. Lett. **102**, 242905 (2013).
[11]M. H. Park, H. J. Kim, Y. J. Kim, T. Moon, and C. S. Hwang, Appl. Phys. Lett. **104**, 072901 (2014).
[12]M. H. Park, H. J. Kim, Y. J. Kim, T. Moon, K. D. Kim, and C. S. Hwang, Adv. Energy Mater. **4**, 1400610 (2014).
[13]M. H. Park, H. J. Kim, Y. J. Kim, T. Moon, K. D. Kim, and C. S. Hwang, Nano Energy **12**, 131 (2015).
[14]J. Müller, U. Schröder, T. S. Böscke, I. Müller, U. Böttger, L. Wilde, J. Sundqvist, M. Lemberger, P. Kücher, T. Mikolajick, and L. Frey, J. Appl. Phys. **110**, 114113 (2011).
[15]T. Olsen, U. Schröder, S. Müller, A. Krause, D. Martin, A. Singh, J. Müller, M. Geidel, and T. Mikolajick, Appl. Phys. Lett. **101**, 082905 (2012).
[16]S. Starschich, D. Griesche, T. Schneller, R. Waser, and U. Böttger, Appl. Phys. Lett. **104**, 202903 (2014).
[17]T. Shimizu, K. Katayama, T. Kiguchi, A. Akama, T. J. Konno, and H. Funakubo, Appl. Phys. Lett. **107**, 032910 (2015).
[18]S. Mueller, J. Mueller, A. Singh, S. Riedel, J. Sundqvist, U. Schroeder, and T. Mikolajick, Adv. Funct. Mater. **22**, 2412 (2012).
[19]S. Mueller, C. Adelmann, A. Singh, S. Van Elshocht, U. Schroeder, and T. Mikolajick, J. Solid State Sci. Technol. **1**, N123 (2012).
[20]T. Schenk, S. Mueller, U. Schroeder, R. Materlik, A. Kersch, M. Popovici, C. Adelmann, S. V. Elshocht, and T. Mikolajick, in *Proceedings of the European Solid-State Device Research Conference* (2013), p. 260.
[21]E. H. Kisi, C. J. Howard, and R. J. Hill, J. Am. Ceram. Soc. **72**, 1757 (1989).
[22]S. E. Reyes-Lillo, K. F. Garrity, and K. M. Rabe, Phys. Rev. B **90**, 140103(R) (2014).
[23]R. Ruh, H. J. Garrett, R. F. Domagala, and N. M. Tallan, J. Am. Ceram. Soc. **51**, 23 (1968).
[24]R. Materlik, C. Künneth, and A. Kersch, J. Appl. Phys. **117**, 134109 (2015).
[25]E. H. Kisi and C. J. Howard, Key Eng. Mater. **153–154**, 1–36 (1998).
[26]J. H. Haeni, P. Irvin, W. Chang, R. Uecker, P. Reiche, Y. L. Li, S. Choudhury, W. Tian, M. E. Hawley, B. Craigo, A. K. Tagantsev, X. Q. Pan, S. K. Streiffer, L. Q. Chen, S. W. Kirchoefer, J. Levy, and D. G. Schlom, Nature **430**, 758 (2004).
[27]A. Christensen and E. A. Carter, Phys. Rev. B **58**, 8050 (1998).
[28]H. N. Lee, S. Senz, A. Pignolet, and D. Hesse, Appl. Phys. Lett. **78**, 2922 (2001).
[29]F. Namavar, G. Wang, C. L. Cheung, R. F. Sabirianov, X. C. Zeng, W. N. Mei, J. Bai, J. R. Brewer, H. Haider, and K. L. Garvin, Nanotechnology **18**, 415702 (2007).
[30]D. Wang, Y. Guo, K. Liang, and K. Tao, Ser. A: Math. Phys. Astron. **42**, 80 (1999).
[31]See supplementary material at http://dx.doi.org/10.1063/1.4939660 for parameters reflecting the strain state, HRTEM image, approximations made in the model, *P-E* results of films with thicknesses of 8, 18, and 24 nm, more discussion on the origins of the disappearance of hysteresis, DC leakage and dielectric behavior of all films, fatigue behavior of the 12-nm-thick film, and XPS spectra of the 12-nm-thick film.
[32]M. H. Park, H. J. Kim, Y. J. Kim, T. Moon, K. D. Kim, Y. H. Lee, S. D. Hyun, and C. S. Hwang, J. Mater. Chem. C **3**, 6291 (2015).
[33]T. Schenk, U. Schroeder, and T. Mikolajick, IEEE Trans. Ultrason. Ferroelectr. Freq. Control **62**, 596 (2015).
[34]T. Schenk, E. Yurchuk, S. Mueller, U. Schroeder, S. Starschich, U. Böttger, and T. Mikolajick, Appl. Phys. Rev. **1**, 041103 (2014).
[35]B. Tadić, Eur. Phys. J. B **28**, 81 (2002).
[36]C. J. Huang, K. Li, S. Y. Wu, X. L. Zhu, and X. M. Chen, J. Materiomics **1**, 146 (2015).
[37]H. Yan, F. Inam, G. Viola, H. Ning, H. Zhang, Q. Jiang, T. Zeng, Z. Gao, and M. J. Reece, J. Adv. Dielectr. **1**, 107 (2011).
[38]X. L. Wang, B. Li, X. L. Zhong, Y. Zhang, J. B. Wang, and Y. C. Zhou, J. Appl. Phys. **112**, 114103 (2012).